

# DIRECT LASER DEPOSITION OF Ti-6Al-4V FROM ELEMENTAL POWDER BLENDS

Lei Yan<sup>1</sup>, Xueyang Chen<sup>1</sup>, Wei Li<sup>1</sup>, Frank Liou<sup>1</sup>, and Joe Newkirk<sup>2</sup>

<sup>1</sup>Department of Mechanical and Aerospace Engineering,  
Missouri University of Science and Technology, Rolla, MO 65409

<sup>2</sup>Department of Materials Science and Engineering,  
Missouri University of Science and Technology, Rolla, MO 65409

REVIEWED

## Abstract

A thin-wall structure composed of Ti-6Al-4V has been deposited using direct laser deposition (DLD) from blended Ti, Al, and V elemental powders. The microstructure and composition distribution along the build height direction were intensively investigated using optical microscopy, scanning electron microscopy/energy dispersive X-ray spectroscopy (SEM/EDS), and Vickers hardness testing. The microstructures of the as-deposited Ti- $x$ Al- $y$ V were studied using EDS to determine appropriate weight percentage for Al and V in the blended powders before mixing. The effects of laser power and laser transverse speed on the microstructure were investigated and optimized laser processing parameters were concluded.

## 1. Introduction

Direct laser deposition (DLD) is a viable and promising technology that has revolutionized manufacturing complex and hard-manufactured material components. DLD manufactured parts are precisely built by adding material layer by layer, usually in powder form. Conventionally, a prealloyed powder, in which each individual powder particle has the composition of the desired alloy composition in the final part, is used in the DLD technique [1]. A different or an improved approach of laser deposition is using mixed elemental powders to flexibly create materials in situ with the development of powder feedstock. With the blends of elemental powders, each individual powder particle has an elemental composition of an element present in the desired final alloy composition. Upon mixing, the sum of all powder particles gives the desired alloy composition in the final part [1]. A variety of materials including metals, alloys, and ceramics have been made with elemental powders such as SS316, titanium-based alloys, nickel-based superalloys Inconel 625, and Fe-Cr-Ni, Fe-Co-Al system alloys [2-8]. Those successes could potentially reduce the costs of processing complex components from powder preparation post-processing to a large extent. In addition, using elemental powder could also benefit the deposition of functionally graded materials (FGM), such as from metal to metal, Ti-V (Mo), and metal-ceramic, Ti-TiC [9-10]. However, only limited studies on Ti-6Al-4V by elemental powder with the DLD method were reported. Present work is focused on processing parameters of laser transverse speed, laser power, and their effects on microstructure, Vickers hardness, and material composition distribution along build height direction.

## 2. Experimental procedures

Thin-wall samples were fabricated at MST laser-aided manufacturing process (LAMP) lab using the DLD system, which consists of an argon-purged chamber, 1 kW Nd-YAG fiber laser,

side nozzle powder feeder, and 3-axis numerical control work table. Fig. 1 shows the experimental set-up of the MST-LAMP DLD system.

Commercially pure Ti, Al, and V powders were weighed out and two sets of powder blends were prepared according to weight percentage ratios of 90:6:4 and 84:8:8 after being dried in the furnace for 30 minutes at 200°C. Two sets of blends were mixed in a sealed bottle using a Turbula® mixer for 10 minutes. The characteristics of the powders are listed in Table 1.

The thin-wall samples were deposited on 2 inches long, ½ inch wide, and ¼ inch thick Ti-6Al-4V substrates. Based on preliminary experiments, laser power from 550 to 750 W, laser transverse speed from 200 to 400 mm/min, the same powder feed rate, and laser beam diameter 3 mm were chosen for the experiments. The experimental design and processing parameters are listed in Table 2.

Cross section of the deposits and substrates were EDM cut, mounted, and then polished according to standard metallographic preparation of Ti-6Al-4V. The samples were etched by Kroll’s reagent consisting of 92 ml distilled H<sub>2</sub>O, 6 ml HNO<sub>3</sub>, and 2 ml HF to reveal α and β phases for further analysis.

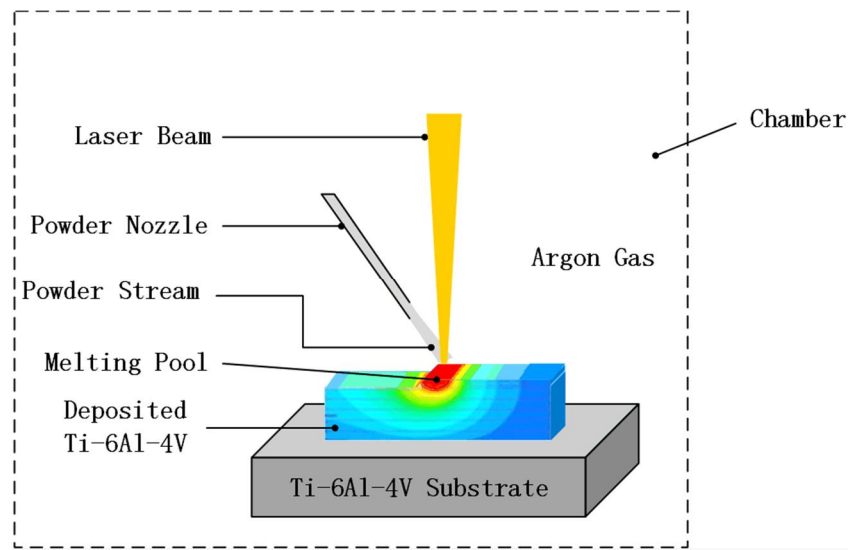


Fig. 1: Schematic of the MST-LAMP DLD system.

Table 1: Powder characters

Powder	Particle Appearance	Particle Size/ $\mu\text{m}$
Ti	irregular	106
Al		165
V		175

Table 2: Experimental design and DLD processing parameters

Sample No.	Power	Scanning Speed (mm/min)	Layer	Layer Thickness (mm)
1	750	200	20	0.2
2	650	400	20	0.2
3	650	300	20	0.2
4	650	200	20	0.2
5	550	200	20	0.2

Vickers hardness was first tested on a Vickers hardness tester with 1 Kg load and 10 seconds dwell time. Vickers hardness sampling points were distributed along three zigzag routes at 0.3 mm intervals and the Vickers hardness at certain positions was taken from the average VHN per each row with the same height. Fig. 2 represents how the Vickers hardness tests were conducted.

The microstructure was studied under the optical microscope (OM) to determine microstructure types and the variation of grain size. The composition distribution along the build height direction was investigated by employing SEM/EDS with Helios 600. Both line scan and area scan were used for the EDS test. For line scan test, lines in the middle of the deposits along the build height direction with length of 160  $\mu\text{m}$  were drawn to detect the homogeneity of material distribution. During area scan tests, 200  $\mu\text{m}$  by 200  $\mu\text{m}$  square areas with center point intervals 300  $\mu\text{m}$  and 500  $\mu\text{m}$  were scanned to determine Ti, Al, and V composition distribution in the as-deposited alloy from top to bottom. The two different intervals 300  $\mu\text{m}$  and 500  $\mu\text{m}$  are for deposits made from powder blends with weight percentage ratio 90:6:4 and 84:8:8 separately. A smaller interval of 300  $\mu\text{m}$  was chosen for short deposit height of the tested samples. A Ti-6Al-4V bulk containing 6.33 Al, 4.10 V, 0.17 Fe, 0.19 O, 0.011 C, 0.013 Cr, 0.012 Ni and 0.02 Si and balanced Ti (all composition in Wt.%) was used as the standard for both line scan and area scan during the EDS tests, which made test accuracy within  $\pm 1\%$  [11].

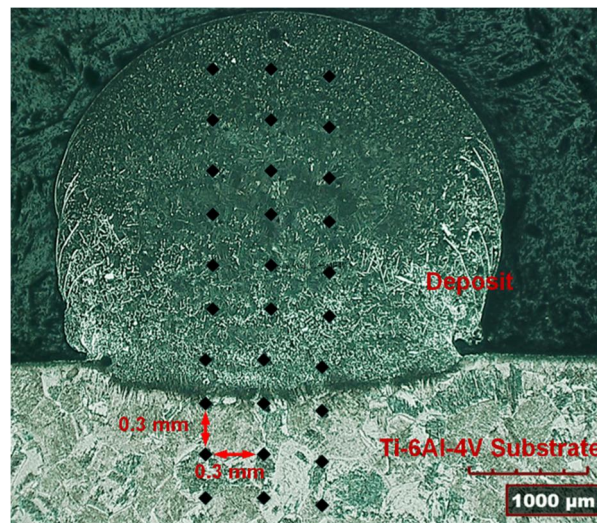


Fig. 2: Vickers hardness test pattern.

### 3. Results and discussion

#### 3.1 Microstructure

Fig. 3 shows the microstructure of DLD Ti-6Al-4V from blended elemental powders with laser transverse speeds 200, 300, and 400 mm/min at a given laser power of 650 W. The microstructure contains primary  $\alpha$ , secondary  $\alpha$  and  $\beta$ . The microstructure varies from bottom to top of the deposits, but a general trend showed the microstructure would be finer closer to the bottom. A steady state was reached from middle to top where not too much difference could be found in the microstructure and basically shows Widmanstätten basketweave, which tends to form with an increasing cooling rate from the  $\beta$ -phase field [12-13].

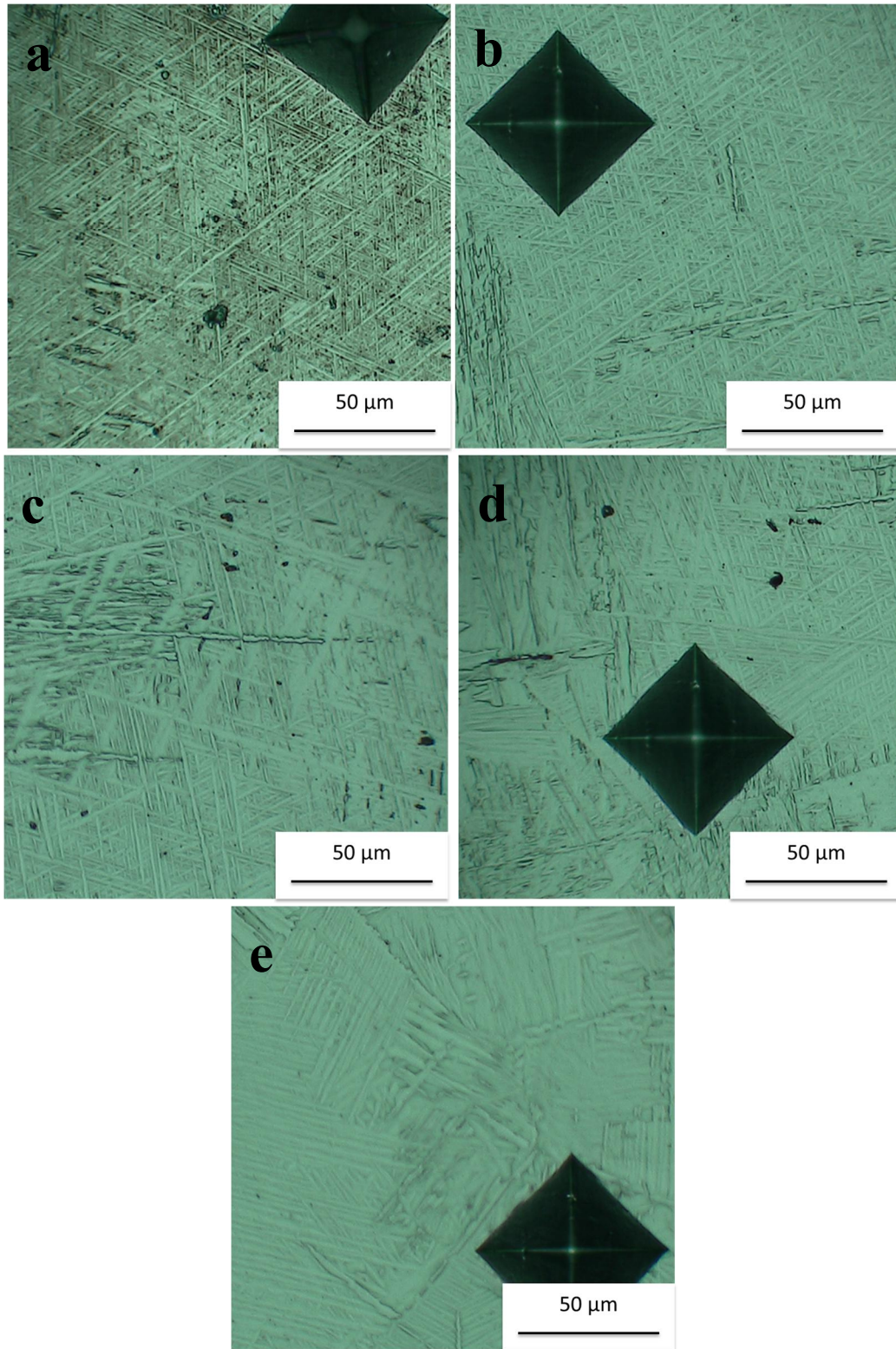


Fig. 3: Microstructure of deposits at laser transverse speed: (a) 200 mm/min, (b) 300 mm/min, (c) 400 mm/min, (d) bottom of deposit at 300 mm/min, (e) top of deposit at 300 mm/min.

The microstructure variation for different laser transverse speed can be explained by the introduced volumetric energy density, which has a high influence on microstructure and its relation

with laser power  $P$  (W), laser transverse speed  $v$  ( $\mu\text{m/s}$ ), hatch spacing  $h$  ( $\mu\text{m}$ ) and layer thickness  $d$  ( $\mu\text{m}$ ). This can be expressed as:  $E = P / (v * d * h)$  [14]. During the experiments, hatch spacing and layer thickness were fixed so increasing laser power and/or decreasing laser transverse speed would increase energy density and leads to a higher cooling rate, which would benefit finer grain formation.

Fig. 3 (a) to (c) shows the basketweave microstructure chosen from the steady state section of three deposits with different laser transverse speed, which reveals that the grain size increased with the laser scanning speed. From the definition of energy density, the higher the laser transverse speed, the lower the cooling rate, which leads to a coarser microstructure [15].

Fig. 3 (d) and (e) shows the microstructure at the bottom and top of the deposit with 300 mm/min laser transverse speed, which reveals that at the lower end of the deposit near the substrate, the grain size was smaller than the upper side. The same trend described above happened at scanning speed 200 mm/min and 400 mm/min, too. The reason was the closer to the substrate, the higher cooling rate happened, and contributed to the formation of finer grains.

Similar phenomenon for laser power 550, 650, and 750 W at fixed laser transverse speed 200 mm/min was observed and the difference between microstructures from different deposits or different positions of the same deposit all could be explained based on the energy density and cooling rate. Therefore, it was concluded that higher laser power and/or slower laser transverse speed tends to benefit the formation of finer microstructures.

### 3.2 Vickers Hardness

The average Vickers hardness values of as-deposited Ti-6Al-4V from blended elemental powders are shown in Fig. 4 to represent Vickers hardness with respect to position in the deposits and the relationship with variations of laser power and laser transverse speed.

Ti-6Al-4V substrate Vickers hardness was first taken near the bottom edge that is away from heat affected zone (HAZ) and the Vickers hardness ranges  $346.47 \pm 9.96$  VHN. It was observed that on the substrate side for each laser transverse speed and laser power, the Vickers hardness values increased when it went into the HAZ. When it goes into the deposit zone, an obvious relationship for both laser transverse speed and laser power with Vickers hardness was observed. Fig. 4 (a) shows Vickers hardness of the deposit at laser power 550 and 650 W doesn't vary too much and almost stayed constant, Vickers hardness varied  $449.64 \pm 7.18$  and  $454.20 \pm 7.10$  VHN, separately. For laser power at 750 W, Vickers hardness ranged  $506.04 \pm 22.52$  VHN and showed an increase from the first several layers, then stayed stable from the middle to the top of the deposit. This is as expected because the higher the laser power, the higher the energy density and higher cooling rate. The higher the cooling rate, the finer the microstructure and which leads to higher Vickers hardness. Fig. 4 (b) reveals the relationship between the laser transverse speed and Vickers hardness. Vickers hardness ranged  $459.04 \pm 9.16$ ,  $454.18 \pm 8.76$ , and  $444.86 \pm 16.74$  VHN for laser transverse speed 200, 300, and 400 mm/min, respectively. Vickers hardness of the three deposits stayed stable at three different laser transverse speeds. It was clear that the decrease in laser transverse speed led to the increase of Vickers hardness and that it also influenced the cooling rate. As the laser transverse speed decreased, energy density and the cooling rate increased. Thus, the lower laser transverse speed was the direct reason for fine grains and higher Vickers hardness.

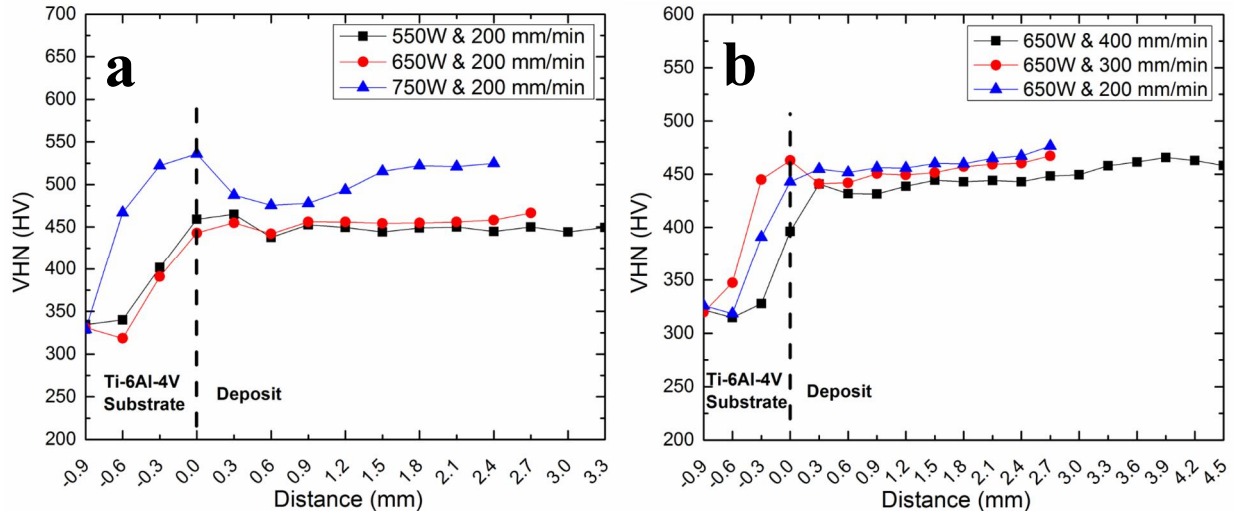


Fig. 4: (a) Vickers hardness vs. laser power, (b) Vickers hardness vs. laser transverse speed.

### 3.3 EDS Test

Ti, Al, and V powders were first mixed with the designated weight percentage ratio of 90:6:4 to get target material Ti-6Al-4V. Area scan and line scan were employed to check the composition distribution along the build height direction. Fig. 5 (a) shows from substrate to top of the deposit Al and V weight percentage decreased and in the opposite direction Ti increased. Al and V curves were zoomed in and show their weight percentage variation against position in Fig. 5 (b). Two marked zones in Fig. 5 (b) mean industry qualified Al and V weight percentage for Ti-6Al-4V, which is Al ranges from 5.5-6.75% and V 3.5-4.5%. At deposit height from 0-0.9 mm only two areas that have the qualified composition weight percentage; this may have been caused by Al and V diffusion from the substrate when the melting pool was generated. Above height 0.9 mm, Al and V weight percentage shows the trend that the values stayed stable around Al 5% and V 2%, which means the as-deposit alloy is actually Ti-5Al-2V and not target material Ti-6Al-4V.

Line scan was also employed during the EDS test to define composition homogeneity along the build height direction. The line scan result in Fig. 5 (c) shows a homogenous chemistry throughout the deposit, but the number of counts doesn't mean an exact measurement of chemistry; the line scan is just a qualitative analysis, but not a quantitative analysis. Improvements could be made by increasing Al and V weight percentage of the blended powders or generating a much bigger melting pool to increase the chance for Al and V powders to fall into.

In order to increase Al and V weight percentage in the deposit, a trial and error method was used and a new weight percentage ratio of 84:8:8 for Ti, Al, and V powers was mixed. Fig. 6 shows the EDS results of the deposit based on the new designed weight percentage ratio. Fig. 6 (a) shows the weight percentage of Al and V slightly increased from the substrate to about 1 mm height and then stayed almost unchanged. Fig. 6 (b) is the zoomed in curves of Al and V and shows that the first 1 mm height of the deposit has qualified Al and V weight percentage and also may diffuse from the substrate via the melting pool. Above 1 mm height, Al and V weight percentage fell into narrow zones 6.75-7% ( $6.9 \pm 0.21\%$ ) and 4.5-5% ( $4.72 \pm 0.10\%$ ), which means the 84:8:8 weight percentage ratio could make Ti- 6.9Al-4.7V and get pretty close to the maximum limit of industry qualified Ti-6Al-4V.

It could be assumed that a little decrease of Al and V content ratio in the mixes from 84:8:8 ratio, such as to 86.5:7:6.5, could get qualified Ti-6Al-4V deposits. The reason for the lack of Al in the deposits may be caused by Al powder's high reflection ratio of the laser beam and lighter

weight compared to Ti and V powders. The lighter weight may lead to Al powder flowing and falling outside the melting pool. Low V weight percentage means less V powder was falling into the melting pool during the deposition process and this may come from the characters of V powder being used during the experiment [16]. V powder's largest particle size and density would cause some of it to fall behind or outside the melting pool and result in the lack of element V. This is a common phenomenon for blended elemental powders, especially when different elemental powders' average particle size and density has significant variation. DLD would benefit from multiple coaxial powder nozzles in this situation [8], which means each nozzle could be set to be perfectly suitable for specific elemental powders to fall into the melting pool.

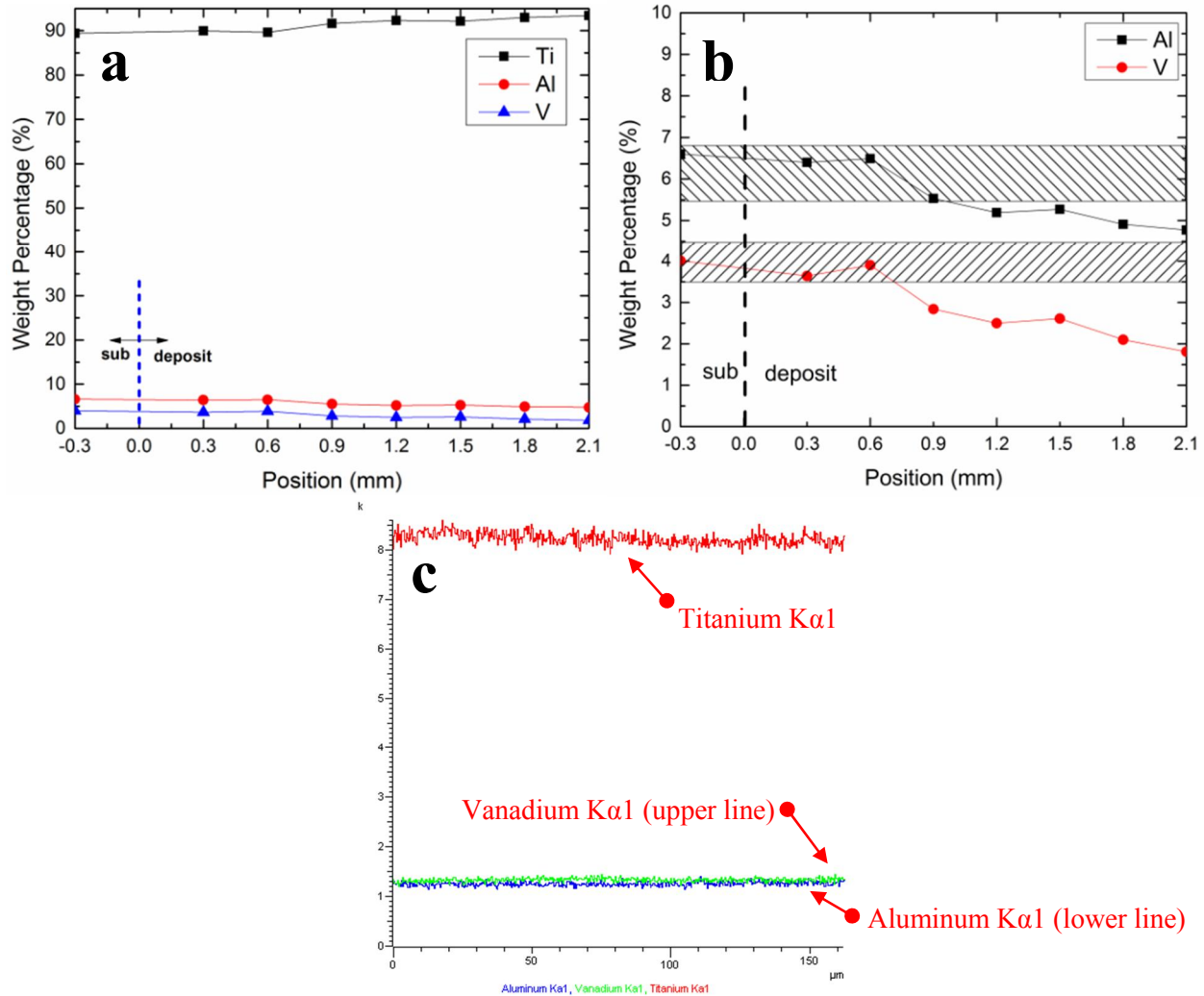


Fig. 5: EDS results for Ti-6Al-4V: (a) Composition distribution along build height direction, (b) zoom in of Al and V curves in Fig. 5 (a), (c) Line scan along build height direction.

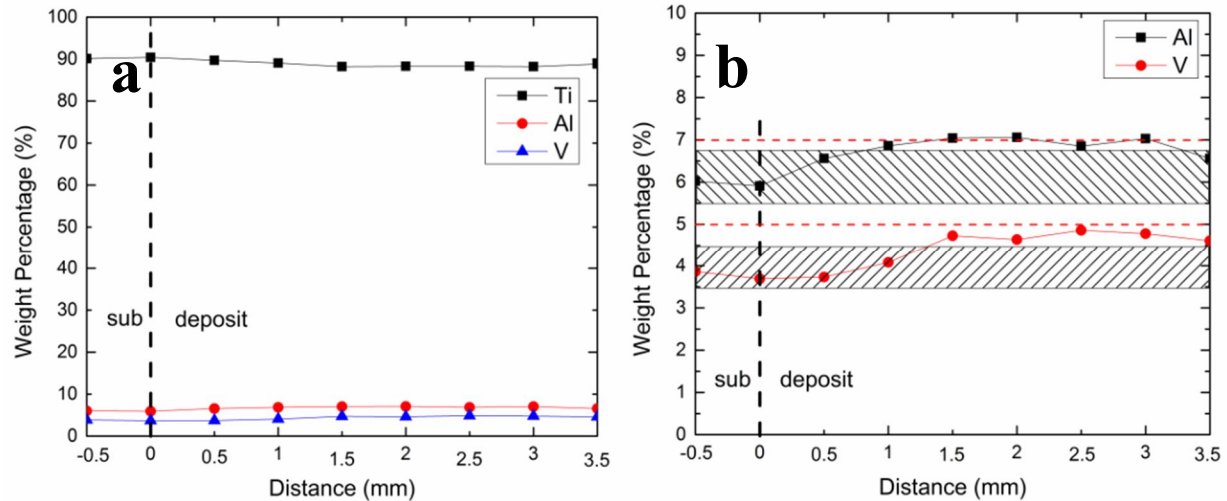


Fig. 6: EDS results for Ti-8Al-8V: (a) Composition distribution along build height direction, (b) zoom in of Al and V curves in Fig. 6 (a).

#### 4. Conclusions

The influence of the laser transverse speed and laser power on microstructure, Vickers hardness, and composition distribution of Ti-6Al-4V made from elemental powder by DLD process were studied. Increasing laser power or decreasing laser transverse speed tended to benefit the formation of finer grains. Vickers hardness is related to grain size, and the finer the grain size, the higher Vickers hardness the material reveals. Thus, increasing laser power or decreasing laser transverse speed increased Vickers hardness. The EDS tests results show that increasing Al and V weight percentage from 6% and 4% of the powder blends to 8% and 8% would increase Al and V weight percentage in the deposit and make it much closer to the industry qualified Ti-6Al-4V.

#### Acknowledgements

This work was conducted as part of NASA's project through EPSCoR Grant #NNX13AM99A. The support from Boeing is also gratefully acknowledged.

#### References

- [1] Clayton, Rodney Michael. The use of elemental powder mixes in laser-based additive manufacturing. 2013.
- [2] Brown, Clyde O., Edward M. Breinan, and Bernard H. Kear. "Method for fabricating articles by sequential layer deposition." U.S. Patent No. 4,323,756. 6 Apr. 1982.
- [3] Keicher, David M., and W. Doyle Miller. "LENSTM moves beyond RP to direct fabrication." *Metal Powder Report* 12.53 (1998): 26-28.
- [4] Lewis, G. K., et al. Los Alamos Technical Report. LA-UR-95-2845, 1995.
- [5] Snow, D. B., E. M. Breinan, and B. H. Kear. "Rapid solidification processing of superalloys using high power lasers." *Champion PA (ed) Proceedings of the conference superalloys*. Vol. 80. 1980.
- [6] Brooks, J., Robino, C., Headley, T., Goods, S., & Griffith, M. (1999). *Proceedings of the Solid Freeform Fabrication* (p. 375). University of Texas, Austin.
- [7] Brice, C. A., Schwendner, K. I., Mahaffey, D. W., Moore, E. H., & Fraser, H. I. (1999). *Proceedings of the Solid Freeform Fabrication* (p. 369). University of Texas, Austin.

- [8] Takeda, T., Steen, W. M., & West, D. R. F. (1984). Proceedings of ICALEO'84 (Vol. 44, p. 151).
- [9] Collins, P. C., et al. "Laser deposition of compositionally graded titanium–vanadium and titanium–molybdenum alloys." *Materials Science and Engineering: A* 352.1 (2003): 118-128.
- [10] Liu, Weiping, and J. N. DuPont. "Fabrication of functionally graded TiC/Ti composites by laser engineered net shaping." *Scripta Materialia* 48.9 (2003): 1337-1342.
- [11] Bob Hafner. *Energy Dispersive Spectroscopy on the SEM: A Primer* [pdf document]. Retrieved from [http://www.charfac.umn.edu/instruments/eds\\_on\\_sem\\_primer.pdf](http://www.charfac.umn.edu/instruments/eds_on_sem_primer.pdf)
- [12] Kelly, S. M., and S. L. Kampe. "Microstructural evolution in laser-deposited multilayer Ti-6Al-4V builds: Part I. Microstructural characterization." *Metallurgical and Materials Transactions A* 35.6 (2004): 1861-1867.
- [13] Fu, Tian, et al. "Microstructural characterization of diode laser deposited Ti-6Al-4V." Missouri University of Science and Technology, Proceedings of the 19th Annual SFF Symposium, Austin, Tx., pp110-115. 2008.
- [14] Simonelli, M., Y. Y. Tse, and C. Tuck. "Microstructure of Ti-6Al-4V produced by selective laser melting." *Journal of Physics: Conference Series*. Vol. 371. No. 1. IOP Publishing, 2012.
- [15] Nassar, Abdalla R., and Edward W. Reutzel. "Additive Manufacturing of Ti-6Al-4V Using a Pulsed Laser Beam." *Metallurgical and Materials Transactions A* 46.6 (2015): 2781-2789.
- [16] Zhang, Fengying, et al. "Composition control for laser solid forming from blended elemental powders." *Optics & Laser Technology* 41.5 (2009): 601-607.